Non-LTE Models of the Emitting Regions in Young Hot Stars

L.V. Tambovtseva[1], V.P. Grinin[1,2]

E-mail: *lvtamb@mail.ru*

Various disk and outflow components of the circumstellar environment of young Herbig Ae/Be stars may contribute to the hydrogen line emission. These are a magnetosphere, disk wind (photoevaporative, magneto-centrifugal, conical or X-wind), gaseous accretion disk (both hot surface layers (inward of 10 AU) and innermost hot midplane of the accretion disk heated by the viscous dissipation (inward of 0.1 AU). Non-LTE modeling was performed to show the influence of the model parameters on the intensity and shape of the line profiles for each emitting region, to present the spatial distribution of the brightness for each component and to compare the contribution of each component to the total line emission. The modeling shows that the disk wind is the dominant contributor to the hydrogen lines compared to the magnetospheric accretion and gaseous accretion disk.

1 Introduction

The star formation theory developed for T Tauri stars (TTSs) successfully explains magnetospheric accretion [1, 2, 3], and magneto-centrifugal disk wind and jet formation [4, 5, 6]. To improve our knowledge of the physical processes in Herbig Ae/Be stars, it is useful to investigate them with theoretical models developed for TTSs, taking into account the special features of HAEBEs (the large luminosity, rapid rotation, weak magnetic fields).

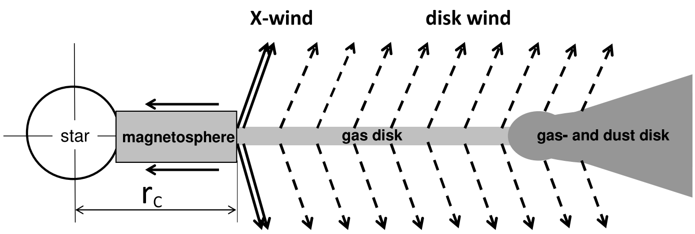

Figure 1: A sketch of line emitting regions in Herbig Ae star.

The promising method to probe the inner environment of young stars is to simultaneously reproduce both the hydrogen emission spectra and the observables of infrared long-baseline interferometry, that is, visibilities, wavelength-differential phases, and closure phases, e.g. [7, 8, 9, 10]. Let us consider

[1] Pulkovo Astronomical observatory, St. Petersburg, Russia
[2] Sobolev Astronomical Institute of St. Petersburg University, Russia

V. Grinin et al. (eds) Radiation mechanisms of astrophysical objects. Yerevan: Edit Print, 2017, pp. 245–252.

schematic picture of the environment of the young intermediate-mass Herbig Ae/Be stars (HAEBEs) (Fig. 1). It presents several gaseous regions emitting the hydrogen lines: (1) magnetospheric accretion region, (2) disk wind which can be presented in the different form (magneto-centrifugal wind, X-wind, conical wind and photoevaporative wind), (3) gaseous accretion disk, and (4) probably polar stellar wind. In this paper, we summarize results of our simultaneous non-LTE modeling of the Brγ emission lines in the spectra of several Herbig Ae/Be stars and interferometric variables obtained for these stars.

1.1 Computational scheme

For all emitting components we performed the non-LTE modeling solving the radiative transfer problem. Differences are in geometry of the regions, and, consequently, in the form of the mass continuity equation and velocity gradient. Solution of the radiative transfer problem has been made as follows. We calculated the excitation and ionization state with the help of numerical codes developed by [11, 12, 13] for the media with the large velocity gradient. The radiative terms in the equations of the statistical equilibrium which take into account transitions between the discrete levels are calculated in the Sobolev approximation [14]. The intensity of the disk wind radiation emergent at the frequencies within the spectral line has been calculated by exact integration over spatial co-ordinates in the approximation of the full redistribution over the frequencies in the co-moving coordinate system. We considered 15 atomic levels and continuum. The

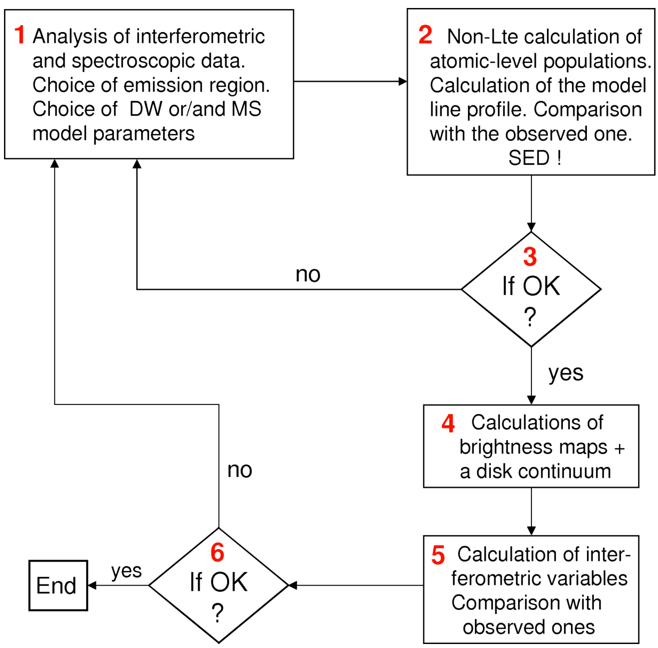

Figure 2: A principle algorithm of simultaneous calculations of emission in the line and interferometric variables.

algorithm of simultaneous calculations of the line emission and interferometric functions is shown in Fig. 2:

1) We choose the appropriate model parameters and compute the velocity and density distribution throughout the region.
2) We divide the integration region by the grid with cells over co-ordinates $[l, \theta, \varphi]$, assuming a wind/accretion temperature distribution. We solve the equation system of statistical equilibrium for the hydrogen atoms in each cell and find the populations of the atomic levels and ionization state in the media.
3) We compare the line profile with the observed one. In the case of a good agreement, we calculate brightness maps at the given frequencies.
4) We calculate the interferometric functions (visibilities, differential and closure phases) and compare them with the observed ones. In the case of the bad agreement we change the model of emitting region. Modeling process is described in details in [15, 16].

2 Models of emitting regions

2.1 Disk wind

Blandford and Payne [17] showed that if an open magnetic field passed through an infinitely thin, Keplerian disk, and is “frozen” into it, and if the field lines make with the disk surface an angle equal to or less than 60°, then gas from the disk surface will be flung out centrifugally along the field lines and can be accelerated to super-Alfvenic velocities. Father from the disk the toroidal component of the field collimates the outflow into two jets which are perpendicular to the disk plane.

There is a method of parametrization where the velocity and temperature distributions can be expressed in a parametric form (see, e.g. [3]). We applied it for HAEBEs. We divide the region of the disk wind by several streamlines, which are going out from point S (Fig. 3). We solve the mass continuity equation for each streamline using a sphere with the center in S. For simplicity, the disk wind consists of hydrogen atoms with a constant temperature ($\sim$10 000 K) along

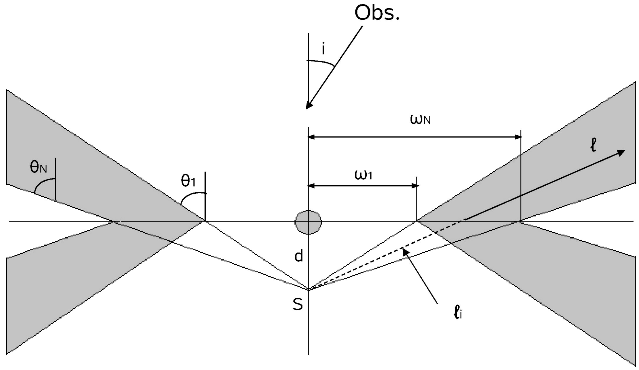

Figure 3: A sketch of the disk-wind region (not to scale).

Table 1: Disk wind model parameters

Model	θ_1	$\omega_1 - \omega_N$	γ	β	$\dot{M}_w$ in $M_\odot$ yr^{-1}
1	30°	$2R_* - 30R_*$	3	4	3×10^{-8}
2	30°	$2R_* - 20R_*$	3	5	3×10^{-8}
3	30°	$2R_* - 20R_*$	3	5	1×10^{-8}

the wind streamlines. As showed by Safier [18], the wind is rapidly heated by ambipolar diffusion to a temperature of ~10 000 K. The wind electron temperature in the acceleration zone near the disk surface is not high enough to excite the Br line emission. Therefore, in our model, the low-temperature region below a certain height value does not contribute to the line emission. A full description of the disk wind model can be found in [15, 7].

Model parameters are as follows: ω_1 and ω_N are foot points of the disk wind launch region for the first and last trajectories of motion, or streamlines, respectively, θ_1 is the half opening angle between the 1st streamline and the vertical axis. The tangential velocity component $u(\omega)$ and poloidal velocity component $v(l)$ change along the streamlines, as given by

$$u(\omega) = u_K(\omega_i)\,(\omega/\omega_i)^{-1}, \tag{1}$$

$$v(l) = v_0 + (v_\infty - v_0)\,(1 - l_i/l)^{\beta}. \tag{2}$$

Here, $u_K(\omega_i) = (G\,M_*/\omega_i)^{1/2}$ at the starting point ω_i, v_0 and v_∞ are the initial and terminal velocities, respectively, G is the gravitation constant, M_* is the stellar mass, and β is a parameter. We assume v_0 to be the sound velocity in the disk wind, $v_\infty = f u_K(\omega_i)$, where $u_K(\omega_i)$ is the Keplerian velocity at distance ω_i from the star, and f is a scale factor. The two last parameters are the mass loss rate $\dot{M}_w$ and γ. The latter regulates the mass loading among the streamlines.

Examples of Hα and $H\beta$ line profiles (model 1 from Table 1) are presented in Fig. 4, where the profiles are shown for inclination angels from nearly pole-on

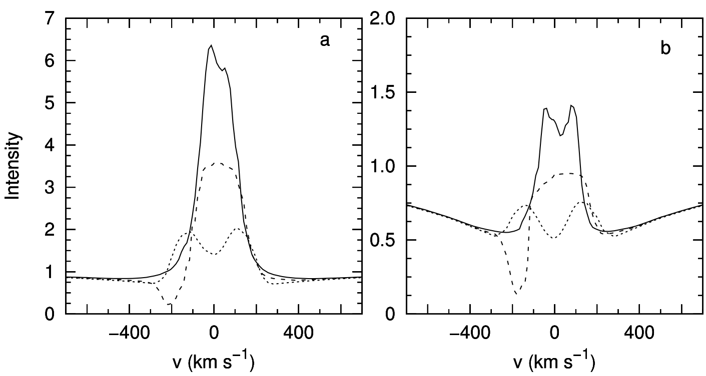

Figure 4: Hα (a) and Hβ (b) line profiles in the disk-wind model 1. Inclination angles are 30° (solid line), 47° (dashed line), and 85° (tiny dashed line); 0° corresponds to the face-on inclination.

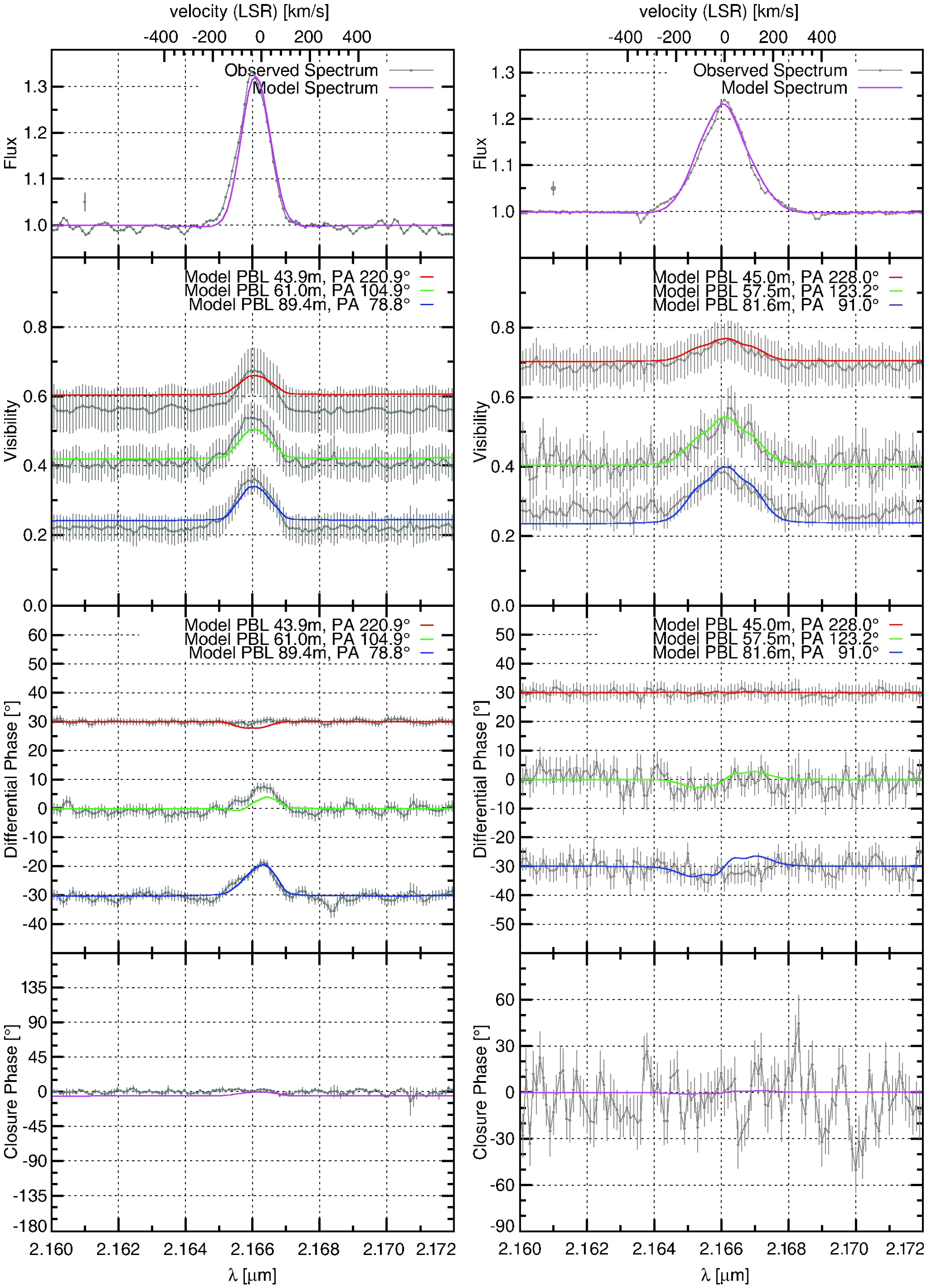

Figure 5: Brγ line profiles and interferometric variables observed and calculated in the framework of the disk wind models for the Herbig Be star HD 98922 (left) and the Herbig Ae star MWC 275 (right).

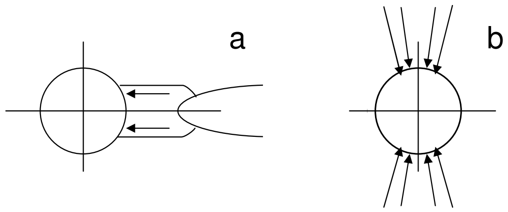

Figure 6: Sketch of the disk (a) and magnetospheric (b) accretion in HAEBEs.

to edge-on view. One can see modification of the line profile from a single one to P Cygni and double-peaked profiles. Modeling with simultaneous calculations of the Brγ line profiles and infrared interferometric variables was performed for several Herbig Ae/Be stars (MWC 297, MWC 275, and HD 98922 – [7, 8, 9]). Details and model parameters can be found in the papers cited. Examples of the observed and calculated line profiles and interferometric functions are presented in Fig. 5.

2.2 Magnetosphere and accretion disk

In our papers [13, 19, 16], we adapted the classical magnetospheric accretion model for TTSs to intermediate-mass Herbig Ae/Be stars. Taking into account that HAEBEs are luminous and rapidly rotating stars, we used a very compact disk-like magnetosphere with rotating gas in free-fall motion (Fig. 6a). This configuration can be used if the stellar magnetic field is weak enough to allow the accreting gas to approach the star surface at the low latitudes. Another configuration of the accreting zone (Fig. 6b) is expected if the magnetic field of the star is strong enough to transport the gas onto the pole regions [20]. In this case we can model the magnetospheric accretion zone by bi-polar thin cones because these regions contribute much more to the hydrogen line emission than outer parts of magnetosphere (not shown in Fig. 6b) due to the smaller gas temperatures in the outer regions. Our calculations of the infrared Brγ line emission (that probes the innermost stellar environment) together with interferometric functions showed that the contribution of the magnetospheric region to the hydrogen emission is no more than 40%. Our conclusion for hydrogen lines (including Balmer lines) is as follows: the emission from the magnetospheric accretion region is able to change the shape of the line profile, for example, to increase the wings of the profile and/or make it asymmetric. In calculations we used the ratio $\dot{M}_w/\dot{M}_{acc} =$ 0.1–0.3 $M_\odot$ yr^{-1}. Many examples of the Hα and Brγ lime profiles can be found in [19, 16].

We also considered the inner gaseous accretion disk as a possible source of the hydrogen emission. For formation of the hydrogen line, the temperature and density of the gas have to be high enough. We considered two components of the inner accretion disk: hot layers of the inner gaseous accretion disk (inward of 10 AU) and the innermost hot midplane of the accretion disk heated by viscous dissipation (inward of 0.1 AU) based on the study by Muzerolle et al. [21]

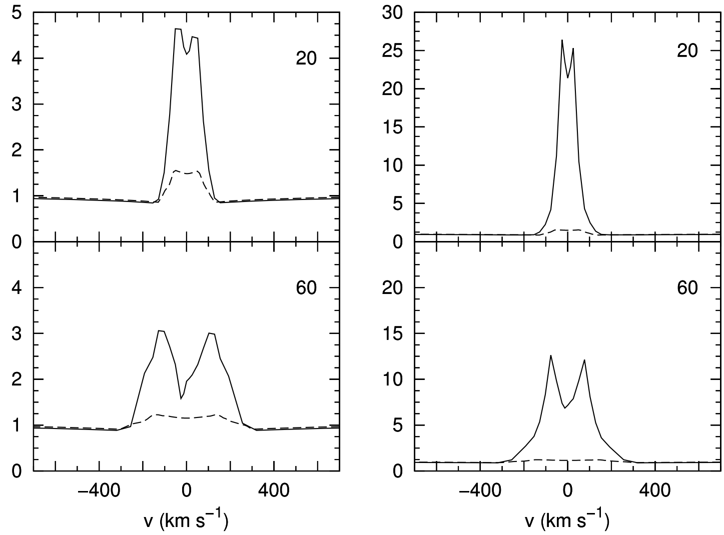

Figure 7: Brγ line profiles in the disk wind models (solid line) and the inner gaseous disk (dashed line) for inclination angles 20° and 60°. *Left*: the disk wind model 2; *right*: the disk wind model 3. Intensities are given in the units of the stellar continuum.

(see details in [16]). All of them contribute *less* Brγ and Hα emission than the *magneto-centrifugal disk*. Several examples of Brγ line profiles from the disk wind and inner gaseous disk are presented in Fig. 7. All they are normalized to the stellar continuum. At these frequencies the disk also emits in the continuum. The profiles for 20° and 60° inclination angles are presented. The same model of the inner disk heated by the viscous dissipation is compared with the disk wind models 2 and 3 from Table 1. Parameters of the disk model are: $R_{in} = 2R_*$, $R_{out} = 10R_*$, $\dot{M}_{acc} = 1 \times 10^{-7} M_\odot\ \mathrm{yr}^{-1}$. The gas temperature is equal to 6000 K near R_{in} and decreases with the distance r. The emission from the hot midplane of the inner gaseous accretion disk can also slightly change the line profile and increase the intensity of the line profile but is substantially less than that from the disk wind.

The hot layers of the inner gaseous accretion disk are not able to contribute strongly into the hydrogen line emission but together with the emission from the outer photoevaporating wind they are able to modify the shape of the line profile, for example, to fill in a small gap between two peaks with additional emission and transform the shape of the profile from double-peaked to single-peaked.

3 Conclusion

Unlike low-mass T Tauri stars, the disk wind of Herbig Ae/Be stars contributes substantially to the hydrogen emission spectra; nevertheless, the region of the magnetosphere is also a source of the emission and has to be taken into account.

Combination of the disk wind parameters and inclination angles permits us to obtain a large variety of profile shapes.

Calculation of the interferometric functions together with the emission lines modeling gives strong constraints to model parameters and provides us with an additional information about the star plus disk system.

Acknowledgments. This research has been supported in part by the Russian Foundation for Basic Research (Projects 15-02-05399 and 15-02-09191).

References

1. *L. Hartmann, R. Hewett, N. Calvet*, Astrophys. J., **426**, 669, 1994.
2. *J. Muzerolle, N. Calvet, L. Hartmann*, Astrophys. J., **550**, 944, 2001.
3. *R. Kurosawa, T.J. Harries, N.H. Symington*, Mon. Not. Roy. Astron. Soc., **370**, 580, 2006.
4. *A. Königl, R.E. Pudritz*, in Protostars and Planets IV. Eds. V. Mannings, A.P. Boss, S.S. Russell. Tucson: Univ. Arizona Press, 2000, p. 759.
5. *J. Ferreira*, Jets from Young Stars. Lect. Not. Phys., No. 723. Berlin: Springer-Verlag, 2007, p. 181.
6. *J. Ferreira, C. Dougados, S. Cabrit*, Astron. Astrophys., **453**, 785, 2006.
7. *G. Weigelt, V.P. Grinin, J.H. Groh et al.*, Astron. Astrophys., **527**, 103, 2011.
8. *R. Garcia Lopez, L.V. Tambovtseva, D. Schertl et al.*, Astron. Astrophys, **576**, A84, 2015.
9. *A. Caratti o Garatti, L.V. Tambovtseva, R. Garcia Lopez et al.*, Astron. Astrophys., **282**, 44, 2015.
10. *I. Mendigutía, W.J. de Wit, R. Oudmaijer et al.*, Mon. Not. Roy. Astron. Soc., **453**, 2126, 2015.
11. *V.P. Grinin, N.A. Katysheva*, Izv. Krym. Astrofiz. Obs. (Bull. Crim. Astrophys. Obs.), **62**, 59, 1980.
12. *V.P. Grinin, A.S. Mitskevich*, Astrophys., **32**, 216, 1990.
13. *L.V. Tambovtseva, V.P. Grinin, B. Rodgers, O.V. Kozlova*, Astron. Rep., **45**, 442, 2001.
14. *V.V. Sobolev*, Moving Envelopes of Stars. Cambridge: Harvard Univ. Press, 1960.
15. *V.P. Grinin, L.V. Tambovtseva*, Astron. Rep., **55**, 704, 2011.
16. *L.V. Tambovtseva, V.P. Grinin, G. Weigelt*, Astron. Astrophys., submitted, 2016.
17. *R.D. Blandford, D.G. Payne*, Mon. Not. Roy. Astron. Soc., **199**, 883, 1982.
18. *P. Safier*, Astrophys. J., **408**, 115, 1993.
19. *L.V. Tambovtseva, V.P. Grinin, G. Weigelt*, Astron. Astrophys., **562**, A104, 2014.
20. *F.H. Shu, J. Najita, E. Ostriker, F. Wilkin*, Astrophys. J., **429**, 781, 1994.
21. *J. Muzerolle, P. D'Alessio, N. Calvet, L. Hartmann*, Astrophys. J., **617**, 406, 2004.